Spectrochimica Acta Part A 89 (2012) 114–118

Contents lists available at SciVerse ScienceDirect

Spectrochimica Acta Part A: Molecular and Biomolecular Spectroscopy

journal homepage: www.elsevier.com/locate/saa

Chemical, spectroscopic characterization, DFT studies and antibacterial activities *in vitro* of a new gold(I) complex with rimantadine

Suelen F. Sucena[a], Raphael E.F. Paiva[a], Camilla Abbehausen[a], Ives B. Mattos[b], Marcelo Lancellotti[b], André L.B. Formiga[c], Pedro P. Corbi[a,*]

[a] *Bioinorganic and Medicinal Chemistry Research Laboratory, Institute of Chemistry, University of Campinas – UNICAMP, P.O. Box 6154, 13083-970 Campinas, São Paulo, Brazil*
[b] *Laboratory of Biotechnology, Institute of Biology, University of Campinas – UNICAMP, Campinas, São Paulo, Brazil*
[c] *Coordination Chemistry Laboratory, Institute of Chemistry, University of Campinas – UNICAMP, Campinas, São Paulo, Brazil*

ARTICLE INFO

Article history:
Received 5 October 2011
Received in revised form
15 November 2011
Accepted 15 December 2011

Keywords:
Gold(I)
Rimantadine
Infrared
NMR spectroscopy
DFT studies
Antibacterial assay

ABSTRACT

A novel gold(I) complex with rimantadine (RTD) was obtained and structurally characterized by a set of chemical and spectroscopic analysis. ^{1}H, ^{13}C and ^{15}N nuclear magnetic resonance (NMR) and infrared (IR) spectroscopic measurements suggest coordination of the ligand to Au(I) through the N atom of the ethanamine group. Theoretical (DFT) calculations confirmed the IR assignments and permit proposing an optimized geometry for the complex. The gold(I)–rimantadine complex (Au–RTD) is soluble in methanol, ethanol, dimethylsulfoxide, acetone and acetonitrile. The preliminary kinetic studies based on UV–vis spectroscopic measurements indicate the stability of the compound in solution. Antibacterial activities of the complex were evaluated by an antibiogram assay. The Au–RTD complex showed an effective *in vitro* antibacterial activity against the *Pseudomonas aeruginosa*, *Escherichia coli* (Gram-negative), and *Staphylococcus aureus* (Gram-positive) bacterial strains.

1. Introduction

Synthesis of metal-based drugs and their applications in pharmacology and medicine have experienced an extraordinary increase since the serendipitous discovery of the antibacterial and antineoplasic activities of cisplatin in the 1960s by Rosenberg et al. [1,2]. Since the discovery of the biological activities of cisplatin, thousands of platinum compounds have been prepared and considered as potential chemotherapeutic agents, although only few of them have entered clinical use. Some examples of cisplatin-like chemotherapeutics are carboplatin and oxaliplatin [3]. Another remarkable example of a metal–organic compound used in medicine is the silver–sulfadiazine complex. This compound, which was first described in the 1940s, has been used topically as an antibacterial agent in the treatment of burns and wounds [4,5]. There are three possible mechanisms for inhibition of bacterial growth by aqueous Ag(I) ions described in the literature: (i) interference with the electron transport system; (ii) DNA-binding; and (iii) interaction with the cell membrane [6,7]. Today, the diversity of metal-based compounds and their uses in medicine covers cancer chemotherapy, antiarthritic and antimicrobial agents, enzymatic inhibitors, and so on [2,8]. Particularly, the pharmacological activities of gold-based compounds have been reported since the Middle Ages. As reported by Sadler and Sue, there were prescriptions of gold compounds used for the treatment of a wide range of diseases in the 8th century [9]. At the present time, several biomedical applications of gold(I) complexes, mainly dealing with the treatment of arthritis, are known. The best example of a gold complex used in the treatment of rheumatoid arthritis is Auranofin [9]. Also, there are reports of biological *in vitro* activities of gold(I) complexes concerning the treatment of cancer, HIV and malaria [9–11].

Due to the growth of bacterial resistance to antibiotics [12], syntheses of new metallopharmaceuticals have also been envisaged in order to find safer and more efficient antibiotics than those currently used in medicine [12–14]. Nevertheless, the success of the development of new metal-based drugs is directly related to the choice of the ligands, since they can lead to changes in the reactivity, bioavailability and stabilization of the oxidation state of the metal in the complex [14]. In our research group, several

Abbreviations: RTD, rimantadine; Au–RTD, gold(I) complex with rimantadine; NMR, nuclear magnetic resonance; HMBC, heteronuclear multiple bond coherence; IR, infrared; UV–vis, ultraviolet–visible; TMS, tetramethylsilane; DMSO, dimethylsulfoxide; CD_3OD, deuterated methanol; DFT, density functional theory; LANL2DZ, Los Alamos National Laboratory – 2nd version on double zeta function; B3LYP, Becke 3-Lee Young Parr functional; PES, potential energy surface; ATCC, American type collection cell; MIC, minimal inhibitory concentration; CAP, chloramphenicol.

* Corresponding author. Tel.: +55 19 35213130; fax: +55 19 35213023.
E-mail addresses: pedrocorbi@yahoo.com, ppcorbi@iqm.unicamp.br (P.P. Corbi).

1386-1425/$ – see front matter © 2011 Elsevier B.V. All rights reserved.
doi:10.1016/j.saa.2011.12.043

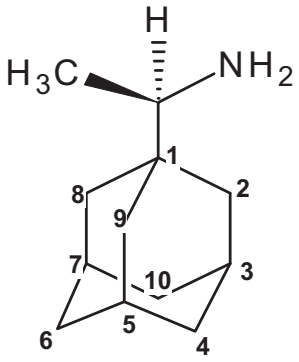

Fig. 1. Structural formula of rimantadine showing carbon atoms numbering.

metal compounds of platinum(II), palladium(II), silver(I) and gold(I) have been synthesized and evaluated as possible antibacterial agents. Among them, gold(I) and silver(I) compounds seem to be the most promising. Special highlights can be given to gold(I)–ibuprofen [12] and gold(I)–mercaptothiazoline complexes [15]. Both compounds have shown to be effective *in vitro* against *Staphylococcus aureus* (Gram-positive), *Pseudomonas aeruginosa* and *Escherichia coli* (Gram-negative) pathogenic bacterial strains. Also, the gold(I) complex with mercaptothiazoline has shown to possess a pronounced cytotoxic activity against HeLa tumorigenic cells, inducing 85% of cell death at a concentration of 2.0 μmol L^{-1} [15].

Diamantoids are defined as a class of hydrocarbons produced by an arrangement of cages formed by sp^3 hybridized carbon atoms [16]. Adamantane (C_6H_{10}) is the simplest representative structure of this class of compounds. Amantadine and rimantadine are examples of organic amines derived from adamantane, and have been considered as pharmaceutical agents. Specifically, rimantadine (RTD, $C_{12}H_{21}N$, Fig. 1) has shown to possess antiviral activity against *Influenza A* virus. This molecule is obtained by functionalization of adamantane with an ethanamine group. Rimantadine seems to act as an M2 ion channel inhibitor, which is responsible for a number of functions, including acidification of the virion [17]. Indeed, the presence of an NH_2 group confers to rimantadine the ability to coordinate metal ions through the nitrogen atom. The present work deals with the synthesis, spectroscopic characterization, DFT studies and antibacterial activities of a novel gold(I) complex with rimantadine (Au–RTD).

2. Experimental

2.1. Materials and equipment

Rimantadine hydrochloride and potassium dicyanoaurate(I), $K[Au(CN)_2]$, were purchased from Sigma–Aldrich Laboratories. Elemental analyses were performed using a PerkinElmer 2400 CHNS Analyzer. Infrared (IR) spectra from 4000 to 450 cm^{-1} were measured using an ABB Bomen MB Series FT-IR spectrophotometer; samples were prepared as KBr pellets. Solution-state ^1H, ^{13}C and ^{15}N nuclear magnetic resonance (NMR) spectra were recorded on a Bruker AVANCE II 400 MHz spectrometer, using a 5 mm probe and at a temperature of 303 K. The ^1H NMR spectrum was acquired at 400 MHz, while the ^{13}C NMR spectrum was acquired decoupled at 100 MHz. Samples were prepared in deuterated methanol (CD_3OD) solutions and the chemical shifts were referenced to TMS. Kinetic studies of the Au–RTD complex were carried out by UV–vis spectroscopic measurements using a Hewlett-Packard 8453A diode array spectrophotometer. A methanolic solution of the complex (6.2×10^{-6} mol L^{-1}) was prepared and measured in 10.00 mm quartz cuvettes. Time intervals of measurements were 30, 60, 120, 180, 240, 300, 360, 420, 480, 540 and 600 min and temperature was maintained constant at 298.0 ± 0.1 K using an Agilent 89090A temperature control device. Thermogravimetric analysis (TGA) was performed on a Simultaneous TGA/DTA SEIKO EXSTAR 6000 Thermoanalyzer, using the following conditions: synthetic air, flow rate of 50 cm^3 min^{-1} and heating rate of 10 °C min^{-1}, from 25 °C to 900 °C. The residue of the thermal treatment was analyzed on a Shimadzu XRD-6000 diffractometer (Cu Kα radiation, λ = 1.5406 Å) with a graphite monochromator and at room temperature. The sample was scanned over the 2θ range from 25° to 80°.

2.2. Synthesis of the complex

The Au–RTD complex was synthesized by the reaction of an aqueous solution of RTD hydrochloride (4.6×10^{-4} mol) with an aqueous solution of potassium dicyanoaurate(I) (4.6×10^{-4} mol) under stirring and at room temperature. After 30 min of constant stirring, the white precipitate obtained was collected by filtration, washed with water and dried over P_4O_{10}. Elemental analysis led to the following molecular formula: $[Au(CN)(C_{12}H_{21}N)]$. Anal. Calcd. for $[Au(CN)(C_{12}H_{21}N)]$ (%): C, 38.8; H, 5.26. Found (%): C, 39.3; H, 4.92. The complex is insoluble in water. It is soluble in methanol, ethanol, dimethylsulfoxide, acetonitrile and acetone. Rimantadine hydrochloride used in the synthesis of the Au–RTD complex is soluble in water, methanol and dimethylsulfoxide. It is insoluble in ethanol, acetone and acetonitrile.

2.3. Molecular modeling

Calculations were carried out using GAMESS [18] software with a convergence criterion of 10^{-4} a.u. in a conjugate gradient algorithm. The LANL2DZ [19] effective core potential was used for gold and the atomic 6-31G(d) basis set for all other atoms [20–23]. Density functional theory (DFT) was performed using B3LYP [24] with a 10^{-5} a.u. convergence criterion for the density change.

2.4. Antibacterial assays

Six pathogenic bacterial strains, *E. coli* ATCC 25922, *P. aeruginosa* ATCC 27853, *P. aeruginosa* 31NM, *S. aureus* ATCC 25923, *S. aureus* BEC9393 and *S. aureus* Rib1, were selected. Bacterial susceptibilities were performed by the diffusion method in accordance with Bauer et al. [25] and confirmed by verification of minimal inhibitory concentration (MIC) as recommended by Clinical and Laboratory Standards Institute (CLSI) [26]. Commercial antibiotic discs of ofloxacin and imipenen were used as positive controls in the disc diffusion experiment. For MIC assays, the standard antibiotic chloramphenicol (CAP) was used as a reference substance.

Stock solutions (10.0 mg mL^{-1}) of Au–RTD and RTD hydrochloride in dimethylsulfoxide were prepared before the experiment. Samples were submitted to serial dilutions (1:1) in a 96 multiplate well with 100 μL of each compound/dilution. Samples were transferred to the plates containing the respective bacterial strain in seven decreasing concentrations.

3. Results and discussion

3.1. Infrared vibrational spectroscopy

The IR spectrum of the Au–RTD complex, presented in Fig. 2a, exhibits a sharp absorption band at 3287 cm^{-1}, which is assigned to the N—H stretching mode. In the RTD hydrochloride spectrum, which is presented in Fig. 2b, the N—H vibration band was observed as a shoulder and with low resolution at 3214 cm^{-1}. According to

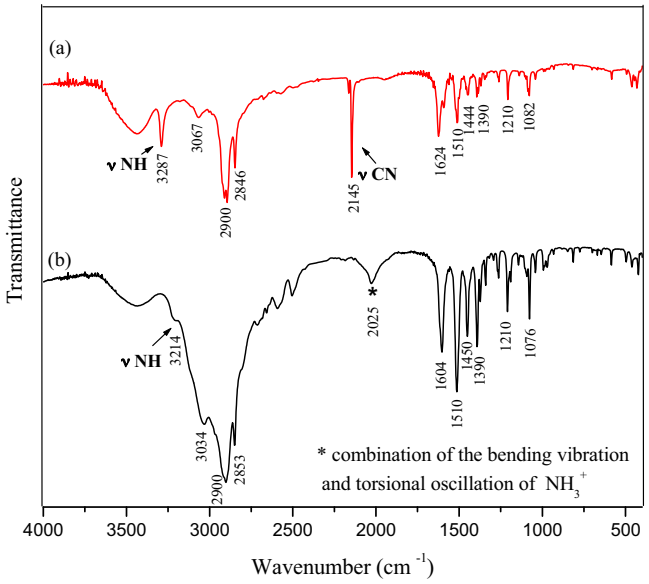

Fig. 2. Infrared vibrational spectra of Au–RTD (a) and RTD (b).

the literature, the shifting of the N–H stretching in the spectrum of the complex when compared to the spectrum of the ligand can be attributed to the coordination of the amino group of RTD to Au(I) [27]. In addition, a combination band at 2025 cm^{-1} was also observed in the IR spectrum of RTD hydrochloride, being assigned to a combination of the asymmetrical NH_3^+ bending vibration and the torsional oscillation of the free NH_3^+ group [28]. The absence of this band in the IR spectrum of the Au–RTD complex is another valuable proof of coordination of NH_2 group to Au(I). Moreover, the IR spectrum of the Au–RTD complex exhibits a strong absorption band at 2145 cm^{-1} which is absent in the IR spectrum of RTD hydrochloride. This band is attributed to the stretching mode of a cyanide group coordinated to Au(I) [18].

3.2. Nuclear magnetic resonance spectroscopy

The ^{13}C and ^{15}N NMR spectra of the Au–RTD and free RTD hydrochloride are shown in Fig. 3. According to the experimental data, changes in chemical shifts are observed for all carbon atoms when the ligand and the complex data are compared, resulting in a $\Delta\delta$ (δ complex $-$ δ ligand) of 1.5 ppm upon coordination. Also, cyanide coordination to gold(I) was confirmed by the presence of the carbon atom of CN group at 150.8 ppm in the ^{13}C NMR spectrum of the compound.

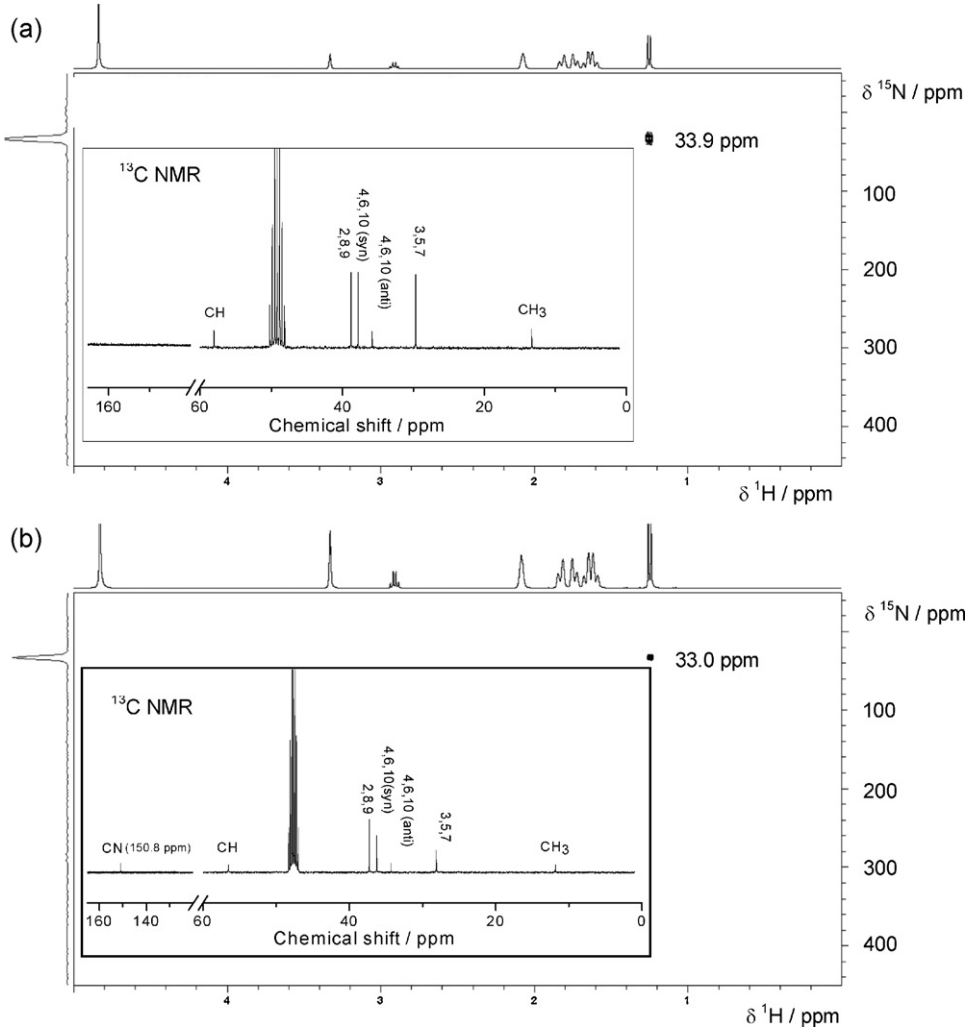

Fig. 3. $^{13}C—\{^1H\}$ (box) and ^{15}N nuclear magnetic resonance spectra of rimantadine hydrochloride (a) and the Au–RTD complex (b).

Table 1
^{13}C and ^{15}N NMR data for RTD and Au–RTD.

Carbon	Chemical Shifts (ppm)	
	RTD	Au–RTD
2,8,9	38.78	37.26
3,5,7	29.66	28.11
4,6,10 (syn)	37.78	36.26
4,6,10 (anti)	35.80	34.30
CH	58.02	56.53
CH_3	13.34	11.85
CN	–	150.8
Nitrogen (NH_2)	33.9	33.0

Coordination of the nitrogen atom of RTD to Au(I) was also evaluated by ^{15}N NMR spectroscopic measurements. The ^{15}N NMR data were indirectly detected from the 2D spectra *via* the heteronuclear [^{1}H—^{15}N] multiple bond coherence technique (HMBC), as described for other metal complexes with N-donor ligands [29,30]. In the RTD hydrochloride spectrum, the ^{15}N chemical shift was observed at 33.9 ppm while for the Au–RTD complex it was observed at 33.0 ppm. The minor isomer shift of ~1.0 ppm may be considered another evidence of coordination of RTD to Au(I) through the N atom. The ^{1}H NMR spectra of the ligand and the complex, including the hydrogen assignments, are also supplied as Supplementary information, while the ^{13}C and ^{15}N NMR data are summarized in Table 1.

3.3. Kinetic studies

The preliminary kinetic data based on the UV–vis spectroscopic measurements show the stability of the Au–RTD complex in solution. The compound did not show changes in the positions or intensities of the UV–vis bands in the time interval of 600 min of analysis, which evidence its stability in the experimental parameters considered in this study.

3.4. Molecular modeling

Theoretical investigations of the coordination of RTD to Au(I) through the nitrogen atom of the NH_2 group were performed in order to confirm the structure of the complex. According to these studies, coordination through nitrogen was confirmed as a minimum of the potential energy surface (PES) with calculations of the Hessians, showing no imaginary frequencies. The calculated structure shows a linear coordination environment for gold as expected for Au(I) complexes with coordination number two. In this case, coordination was shown to occur through the nitrogen atom of rimantadine and also through the carbon atom of the cyanide group. The main calculated bond distances are Au—N 1.95 Å and Au—CN 1.97 Å, while calculated angles are Au—N—C 108.9°, N—Au—C 179.1° and N—C—CH_3 108.9°. The observed Au—CN bond distance is comparable to the experimental data described for other gold(I) cyanide derivatives, where Au—CN bond distance was 1.96 Å [31], and also to the obtained data for the Au–MTZ complex previously reported, where calculated Au—N and Au—CN bond distances were 2.11 Å and 1.98 Å, and calculated N—Au—C was 179° [15].

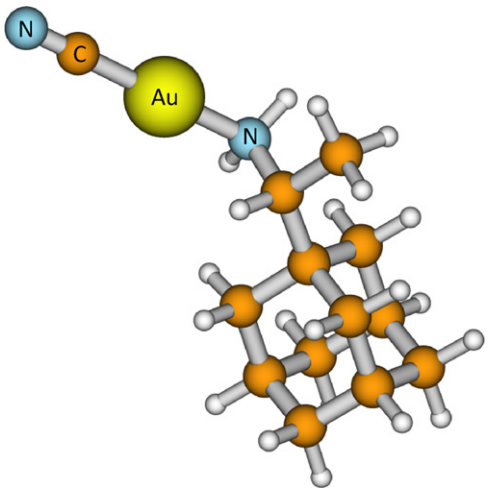

Fig. 4. Optimized structure of the Au–RTD complex.

The analysis of simulated IR data of the ligand and the Au–RTD complex predicts a 90 cm^{-1} positive shift in the N—H symmetric stretching mode of the NH_2 group upon coordination of rimantadine to Au(I). The theoretical results are in a good agreement with the experimental data since the symmetric N—H vibration shows a 73 cm^{-1} positive shift when the ligand and the complex spectra are compared (see Fig. 2).

As described in the literature, when —NH_2 or —NH_3^+ groups make hydrogen bonds, a negative frequency shift and a broadening of the symmetric N—H stretching are expected [32]. In the case of the Au–RTD complex, nitrogen coordination of the NH_2 group to Au(I) leads to the loss of hydrogen bonds, which is consistent with the observed positive frequency shift and narrowing of the symmetric N—H stretching mode as observed in Fig. 2. Finally, for a comparative analysis, the simulated and experimental IR spectra of the Au–RTD complex are presented as Supplementary material.

3.5. Thermal analysis

Thermogravimetric data shows that decomposition of the [Au(CN)($C_{12}H_{21}N$)] complex starts at 155 °C. Rimantadine is lost in the first step of the thermogravimetric curve in the range 155–240 °C (Anal. Calcd. for $C_{12}H_{21}N$ loss 44.6%. Found: 46.5%). Subsequently, the cyanide group is lost in the range 250–500 °C leading to the formation of the final residue (Anal. Calcd. for CN loss: 6.5%. Found: 5.4%). The final residue of thermal treatment was identified by powder X-ray diffraction studies as Au° [33]. The mass loss profile and the X-ray diffractogram of the residue are also supplied as Supplementary material.

3.6. Antibacterial assays

An antibiogram assay was carried out in order to evaluate the antibacterial activities of the Au–RTD complex. The activities of complex against the considered bacterial strains were confirmed by MIC values between 6.25 μg mL^{-1} and 100.0 μg mL^{-1}. The results obtained show promising antibacterial activity of the Au–RTD

Table 2
Antibiotic sensitive profile of bacterial strains against Au–RTD complex and chloramphenicol (CAP).

Compound	Minimal inhibitory concentration (μg mL^{-1})					
	S. aureus BEC 9393	*S. aureus* Rib 1	*S. aureus* ATCC 25923	*P. aeruginosa* ATCC 27853	*P. aeruginosa* 31NM	*E. coli* ATCC 25922
Au–RTD	6.25	6.25	25.0	100.0	100.0	50.0
CAP	–	–	–	50.0	12.5	3.125

complex, being comparable to the inhibitory effect of the standard antibiotics ofloxacin and imipenem used as positive controls, and less active than the standard antibiotic chloramphenicol in the MIC assays for *P. aeruginosa* ATCC 27853, *P. aeruginosa* 31NM and *E. coli* ATCC 25922. The observed results are also comparable to a novel gold(I)–mercaptothiazoline complex, [AuCN($C_3H_5NS_2$)], recently published in the literature [15]. Rimantadine hydrochloride did not exhibit antibacterial activity under the same experimental conditions. Antibiotic sensitivity profiles of bacterial strains are listed in Table 2.

4. Conclusions

A new gold(I) complex with rimantadine of molar composition 1:1 metal/ligand was obtained and characterized. The ^{1}H, ^{13}C and ^{15}N NMR data, in addition to the IR spectroscopic measurements, support coordination of rimantadine to Au(I) through the nitrogen atom of NH_2 group and also through the carbon atom of cyanide. Initial kinetic studies have demonstrated the stability of the compound in solution. Thermal decomposition of the complex starts at 155 °C, leading to the formation of Au° as the final residue of the thermal treatment. DFT studies confirmed coordination of RTD to Au(I) through the nitrogen atom of the NH_2 group as a minimum of the potential energy surface with calculations of the Hessians, showing no imaginary frequencies.

Based on the chemical, spectroscopic and DFT studies the following structure for the Au–RTD complex is proposed in Fig. 4.

Biological studies revealed the effective antibacterial activity *in vitro* of the complex against Gram-negative and -positive bacterial strains. Further studies are envisaged in order to evaluate the *in vivo* antibacterial activities of the Au–RTD complex and its possible application in the treatment of skin infections.

Acknowledgments

This study was supported by grants from FAPESP (2006/55367-2, 2008/56777-5) and CNPq (575313/2008-0 and 472768/2010-3). Authors are also grateful to Professor Carol H. Collins for English revision of the manuscript.

Appendix A. Supplementary data

Supplementary data associated with this article can be found, in the online version, at doi:10.1016/j.saa.2011.12.043.

References

[1] R. Rosenberg, L. Van Camp, T. Krigas, Nature 205 (1965) 698–699.
[2] R. Bakhtiar, E.I. Ochiai, Gen. Pharmacol. 32 (1999) 525–540.
[3] M.A. Jakupec, M. Galanski, V.B. Arion, C.G. Hartinger, B.K. Keppler, Dalton Trans. (2008) 183–194.
[4] G.G. de Gracia, Burns 27 (2001) 67–74.
[5] H.J. Klasen, Burns 26 (2000) 131–138.
[6] K. Nomiya, H. Yokoyama, Dalton Trans. 12 (2002) 2483–2490.
[7] R.B. Thurman, C.P. Gerba, Crit. Rev. Environ. Control 18 (1988) 295–315.
[8] N. Farrell, Coord. Chem. Rev. 232 (2002) 1–4.
[9] P.J. Sadler, R.E. Sue, The chemistry of gold drugs, Metal-Based Drugs (1994) 107–144.
[10] L.L. Marques, G.M. Oliveira, E.S. Lang, M.M.A. Campos, L.R.S. Gris, Inorg. Chem. Commun. 10 (2007) 1083–1087.
[11] A.J. Canumalla, N. Al-Zamil, M. Phillips, A.A. Isab, C.F. Shaw III, J. Inorg. Biochem. 85 (2001) 67–76.
[12] A.T.M. Fiori, W.R. Lustri, A. Magalhães, P.P. Corbi, Inorg. Chem. Commun. 14 (2011) 738–740.
[13] R. Noguchi, A. Hara, A. Sugie, K. Nomiya, Inorg. Chem. Commun. 9 (2006) 355–359.
[14] S. Ray, R. Mohan, J.K. Singh, M.K. Samantaray, M.M. Shaikh, D. Panda, P. Ghosh, J. Am. Chem. Soc. 129 (2007) 15042–15053.
[15] C. Abbehausen, J.F. Castro, M.B.M. Spera, T.A. Heinrich, C.M. Costa-Neto, W.R. Lustri, A.L.B. Formiga, P.P. Corbi, Polyhedron 30 (2011) 2354–2359.
[16] Y. Luzinova, G.T. Dobbs, R. Sassen, B. Mizaikoff, Org. Geochem. 40 (2009) 1143–1150.
[17] S.D. Cady, J. Wang, Y. Wu, W.F. Grado, M. Hong, J. Am. Chem. Soc. 133 (2011) 4274–4284.
[18] M.W. Schmidt, K.K. Baldridge, J.A. Boatz, S.T. Elbert, M.S. Gordon, J.H. Jensen, S.K.N. Matsunaga, K.A. Nguyen, S. Su, T.L. Windus, M. Dupuis, J.A. Montgomery Jr., J. Comput. Chem. 14 (1993) 1347–1363.
[19] P.J. Hay, W.R. Wadt, J. Chem. Phys. 82 (1985) 270–283.
[20] P.C. Hariharan, J.A. Pople, Theor. Chim. Acta 28 (1973) 213–222.
[21] R. Ditchfie, W.J. Hehre, J.A. Pople, J. Chem. Phys. 54 (1971) 720–723.
[22] W.J. Hehre, R. Ditchfield, J.A. Pople, J. Chem. Phys. 56 (1972) 2257–2261.
[23] M.M. Francl, W.J. Pietro, W.J. Hehre, J.S. Binkley, M.S. Gordon, D.J. DeFrees, J.A. Pople, J. Chem. Phys. 77 (1982) 3654–3665.
[24] C. Lee, W. Yang, R.G. Parr, Phys. Rev. B 37 (1988) 785–789.
[25] A.W. Bauer, W.M.M. Kirby, J.C. Sheris, M. Turck, Am. J. Clin. Pathol. 45 (1966) 493–496.
[26] Clinical and Laboratory Standards Institute (CLSI), Performance Standards for Antimicrobial Susceptibility Testing, Seventeenth Informational Supplement, Wayne, PA, USA, 2007.
[27] K. Nakamoto, Infrared and Raman Spectra of Inorganic and Coordination Compounds, Part B, Fifth ed., John Wiley & Sons, New York, 1997.
[28] R.M. Silverstein, F.X. Webster, D.J. Kiemle, Spectrometric Identification of Organic Compounds, Seventh ed., John Wiley & Sons, New York, 2005.
[29] P.P. Corbi, A.C. Massabni, Spectrochim. Acta A 64 (2006) 418–419.
[30] P.P. Corbi, F. Cagnin, L.P.B. Sabeh, A.C. Massabni, C.M. Costa-Neto, Spectrochim. Acta A 66 (2007) 1171–1174.
[31] K.J. Kristopher, R.E. Wasylishen, Inorg. Chem. 48 (2009) 2316–2332.
[32] J.A. Bonacin, A.L.B. Formiga, V.H.S. de Melo, H.E. Toma, Vib. Spectrosc. 44 (2007) 133–141.
[33] Powder Diffraction Database – CD ROM, File 04-0784, The International Centre for Diffraction Data (JCPDS-ICDD) (1997).